Check for updates

Engineering Notes

Rotary Space Tether System for Active Debris Removal

Valeriy I. Trushlyakov*
Omsk State Technical University, 644050, Omsk, Russia
and
Vadim V. Yudintsev†
Samara National Research University, 443086, Samara, Russia

DOI: 10.2514/1.G004615

Downloaded by MCMASTER UNIVERSITY on September 28, 2019 | http://arc.aiaa.org | DOI: 10.2514/1.G004615

Nomenclature

c_t	=	stiffness of the tether, N/m
d_t	=	damping coefficient of the tether, (N · s)/m
l	=	tether length, m
l_0	=	free length of the tether, m
m_1, J_1	=	mass (kg) and moment of inertia of the space tug, kg · m^2
m_2, J_2	=	mass (kg) and moment of inertia of the debris object, kg · m^2
P	=	tug's thrust, N
R	=	distance from the center of the Earth to the center mass of the system, m
$\boldsymbol{R}$	=	column vector of the system's center of mass relative to the Earth, rad
R_e	=	mean radius of the Earth
$\boldsymbol{R}_{A1}$	=	column vector of the tether attachment point on the space tug relative to the Earth's center, m
$\boldsymbol{R}_{A2}$	=	column vector of the tether attachment point on the space debris relative to the Earth's center, m
$\boldsymbol{R}_1$	=	column vector of the space tug relative to the Earth's center, m
$\boldsymbol{R}_2$	=	column vector of the debris relative to the Earth's center, m
T	=	kinetic energy of the system, J
ϑ	=	true anomaly angle, rad
μ	=	gravitational parameter of the Earth
φ_1	=	angle between the tether and space tug, rad
φ_2	=	angle between the tether and space debris, rad
ψ	=	angle between the tether and local vertical axis of the center of mass of the system, rad

I. Introduction

LARGE objects like orbital stages, boosters, and nonfunctional satellites are potential sources of orbital debris that pose a serious hazard to active satellites. To reduce the risk of huge increase in the numbers of debris objects, large objects should be removed from orbits [1,2]. Several space debris removal methods have been proposed in the past years [3–8]. Space tethers are considered as one of the methods for safe transportation of large space debris objects using space tugs [9–14]. A space tug is a spacecraft that can capture and de-orbit a selected space debris object. To capture the debris the space tug should be equipped with a gripping device like single or multiple robotic arms, tentacles, harpoon, and net. Contactless capturing methods also can be used [15–17]. Shan et al. [18] provide review and comparison of the existing technologies on active space debris capturing and removal.

For a robotic arm or any other *stiff* capturing methods, the connection between the tug and debris (target) is stiff, which makes the whole system stable in terms of the relative position of its parts, which is important for control of the system by the space tug. Stiff capturing methods allow using the conventional design of the space tug with the payload section in front of space tug and the thruster section at the rear side (Fig. 1a). The main advantage of this design is that the existing upper stages can be used as space tugs for active debris removal using fuel residuals after the end of the main mission. Figure 1 shows "Fregat"-like orbital stage (space tug) that captures an upper-stage-type debris object using the installed robotic arms as a piggyback payload. The space tug captures the debris using the robotic arms (Fig. 1a) and transfers the debris to the graveyard orbit or to the Earth atmosphere using a push scheme when the tug's thrust $\boldsymbol{P}$ is applied in the direction of the debris object (Fig. 1b).

Capturing of tumbling debris objects using stiff methods is a challenging task. The ability to capture tumbling debris objects leads to an increase in the mass and cost of the gripping device. To overcome these drawbacks, flexible connection capturing methods are proposed in which the debris object and space tug are connected by a tether [19]. The tethered connection between the debris and space tug can be established using flexible devices like nets [20–22] or harpoons [23]. These techniques imply that the space tug *pulls* the debris object with the tether. In the other words, the acceleration of the center of mass of the system ($\boldsymbol{a}_c$) is directed from the center of mass to the space tug (Fig. 2).

This pull technique leads to other problems. For example, for a high-thrust de-orbit maneuver, the tethered tug–debris system's postburn collision between the debris and space tug should be avoided. Jasper and Schaub [24] propose control of the tug's thrust for significantly reducing the postburn relative motion between the tug and debris. Another problem is that the pull scheme constraints the configuration of the space tug, requiring the location of the tether attachment point and tug's propulsion system on the same side of the space tug. The thruster's exhaust in this configuration can damage the tether (Fig. 3a) during possible attitude motions of the space tug. Existing upper stages cannot be used as space tugs with this technique.

In this paper, we present an alternative solution that allows using the push scheme by space tug for orbital transfer of the tethered space debris object. The proposed solution is based on the rotation of the system that induces centrifugal forces that keep the tether taut.

Rotating tethers are considered by DeCou [25] for creating an orbiting stellar interferometer by three satellites at the corners of an equilateral triangle and connecting them by three tethers. Palmerini et al. [26] considered an orbiting, two-dimensional web made by light, flexible tethers. The authors analyzed a simplified rotating web in order to evaluate the spinning velocity able to satisfy the requirement for the stability of the system. In these papers, rotation is used to keep the desired formation of satellites. The presented technique uses tether rotation to apply the tug's thrust along the tether in the direction to the space debris object (Figs. 3a and 3b) changing the motion of the system.

Received 27 May 2019; revision received 21 August 2019; accepted for publication 29 August 2019; published online 26 September 2019. Copyright © 2019 by the American Institute of Aeronautics and Astronautics, Inc. All rights reserved. All requests for copying and permission to reprint should be submitted to CCC at www.copyright.com; employ the eISSN 1533-3884 to initiate your request. See also AIAA Rights and Permissions www.aiaa.org/randp.

*Professor, Department of Aircraft and Rocket Engineering, 11, pr. Mira.
†Associate Professor, Theoretical Mechanics Department, 34, Moskovskoye shosse.

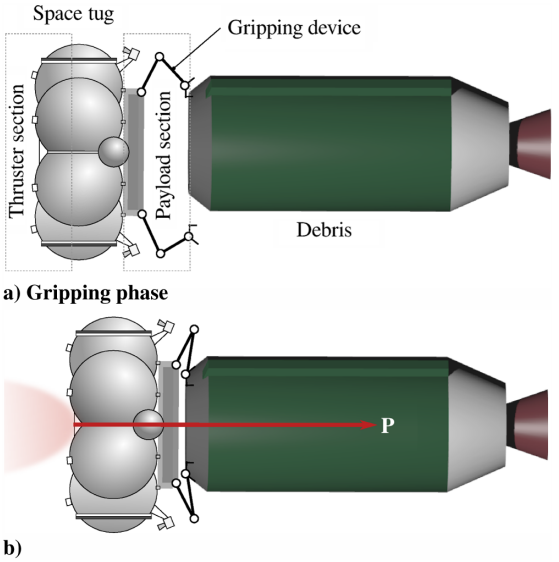

Fig. 1 Gripping the debris object using the stiff method (multiple robotics arms).

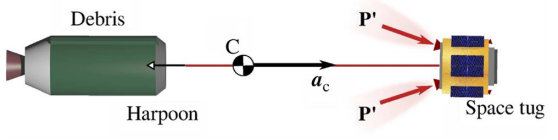

Fig. 2 Pull scheme.

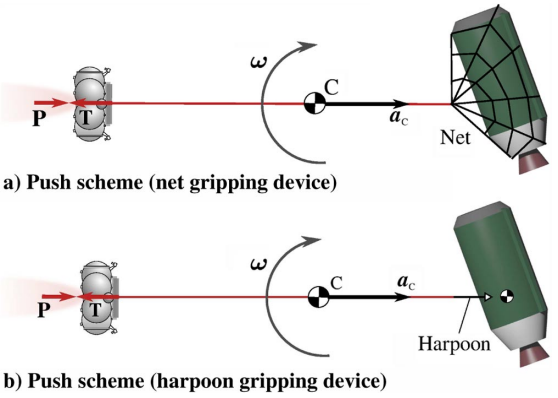

Fig. 3 Push schemes.

Figures 3a and 3b show two possible configurations of the tethered tug–debris system. In the first case, the space debris object is captured using a net. In the second case, the space tug captures the debris using a harpoon device. In both cases, the connection between the tug and debris is nonstiff but the rotation of the tethered tug–debris system allows applying the tug's thrust along the tether.

The next part of the paper consists of three sections. In Sec. II, the idea of the proposed technique and the stages of the active debris removal mission using the autonomous docking module are presented. In Sec. III, the mathematical models of the tethered tug–debris system are described. In Sec. IV, the feasibility of the proposed method is demonstrated through numerical simulation.

II. Rotary Tethered Tug–Debris System

A. Autonomous Docking Module

The proposed technique allows using existing orbital stages as space tugs for active debris removal after the end of the main mission, and so the debris removal mission can be designed as a piggyback mission. In this case, it would be a sound practice to delegate all specific debris removal tasks from the upper stage to a special

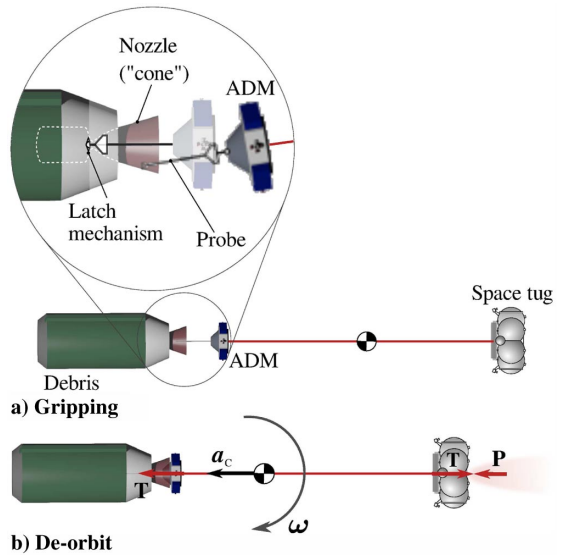

Fig. 4 Active debris removal using the tethered tug–debris system with ADM.

autonomous docking module (ADM) [27–29]. ADM is a small spacecraft that carries all specific equipment for active debris removal mission, including a capture device, control system, and six-degree-of-freedom propulsion system for proximity operations. ADM is delivered by the orbital stage in the proximity of the selected debris object. The ADM separates from the upper stage and captures the debris. ADM can use harpoon or net to capture the debris or use the traditional probe-cone mechanism to dock with the upper-stage-type debris object using the nozzle of the debris as a docking port [30] (Fig. 4). Using of ADM allows reducing demands to the space tug in terms of accuracy of the proximity operations near the space tug.

B. Stages of the Active Debris Removal Mission

Figure 5 shows the main idea of the proposed technique and stages of the active debris removal mission using the ADM. Let us suppose that the space debris object is orbiting a circular orbit of radius R_{deb} and the space tug is orbiting a circular orbit of radius R_{tug}. The proposed technique assumes the following steps of the active debris removal mission (Fig. 5):

1) Transfer of the space tug to the intercept orbit with the perigee $R_p = R_{\text{tug}}$ and the apogee $R_a = R_{\text{deb}} - l_0$, where l_0 is the initial length of the kilometer-order length tether

2) Separation of the ADM from the space tug

3) Gripping the debris object

4) Applying the series of de-orbit impulses along the tether

On the first stage the space tug is transferred to the intercept orbit. The space tug carries the ADM as a piggyback payload with a gripping device like a net, probe-cone mechanism, or harpoon. In the second stage the ADM separates from the space tug for short-range proximity and capturing operations.

The required initial angular rate of the tethered system can be achieved by the relative orbital motion of the space tug and debris at the final approach point (stage 3) when the distance between the space tug and debris is equal to l_0. The space tug and debris have different orbital velocities (V_{tug} and V_{deb}, respectively), which are perpendicular to the tether, and so the initial angular rate of the system is $\omega_0 = (V_{\text{deb}} - V_{\text{tug}})/l_0$. The rotation of the tether with two masses induces the tension force T in the tether that depends on the angular rate of the system ω, tether length l_0, and the masses of the debris m_2 and space tug m_1.

$$T = \omega^2 l \frac{m_1 m_2}{m_1 + m_2} \tag{1}$$

The tension force T allows applying tug's thrust P along the tether to compress it. It is obvious that the tug's thrust P has to be less than the tension force with some margin $P < T$ (see Sec. III).

Downloaded by MCMASTER UNIVERSITY on September 28, 2019 | http://arc.aiaa.org | DOI: 10.2514/1.G004615

Downloaded by MCMASTER UNIVERSITY on September 28, 2019 | http://arc.aiaa.org | DOI: 10.2514/1.G004615

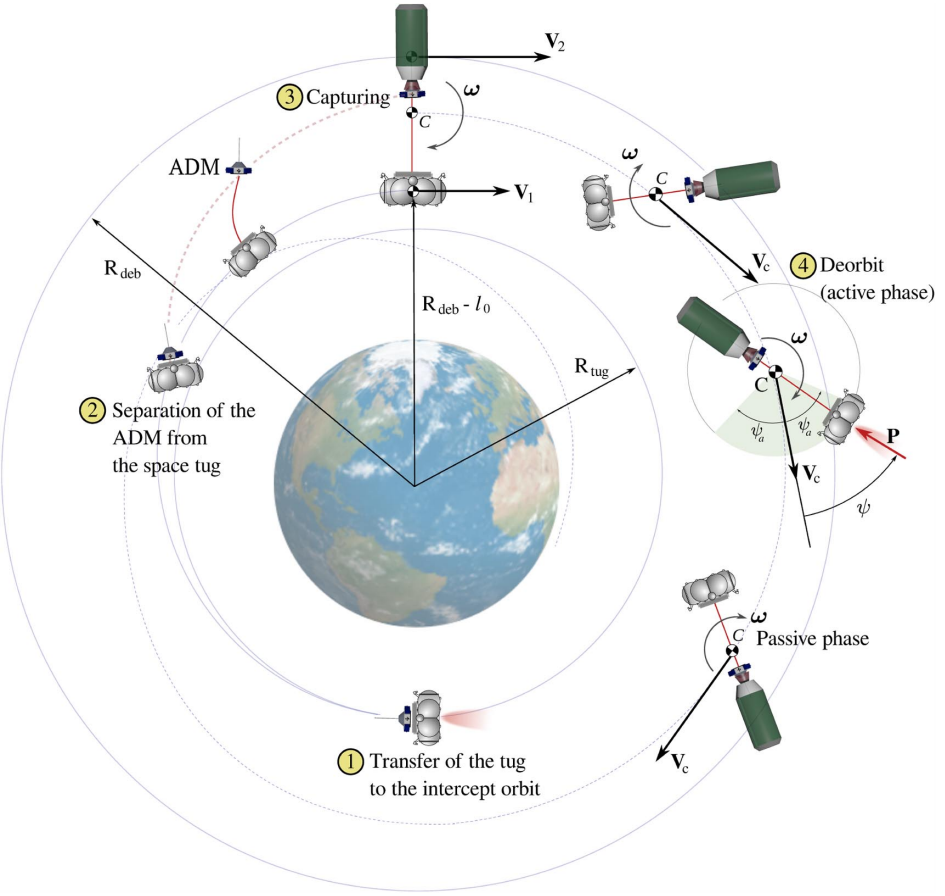

Fig. 5 Stages of the active debris removal mission using the rotating tethered tug–debris system.

Because of the rotation of the tethered tug–debris system the orientation of the tug changes with time. To decrease the orbital height of the system for de-orbiting the tethered debris object, the tug's thrust should be turned on when the cosine of the angle ψ is positive. Angle ψ is the angle between the orbital velocity vector $\boldsymbol{V}_c$ of the tug–debris system and the inverse direction of the tug's thrust vector $\boldsymbol{P}$. So, to decrease the height of the orbit, the tug's thrust should be turned "on" when $\cos\psi > 0$. For more efficient use of the tug's propellant the last condition can be rewritten as $\cos\psi > \cos\psi_a$, $\psi_a \leq \pi/2$. And the angle ψ_a can be found in terms of fuel consumption and de-orbit time. In this paper we do not consider this problem.

To reduce fuel consumption for a de-orbiting mission the tug's thrust can be burned near the apogee of the orbit when (Fig. 6)

$$R \geq R_a - \Delta R_a, \qquad \Delta R_a > 0 \tag{2}$$

where ΔR_a is the maximum difference between the apogee radius of the osculating orbit and radius of the current position of the system that denotes the boundaries of the "active arc" of the orbit where the tug's thruster can be turned "on" if the conditions $\cos\psi > \cos\psi_a$ and $\psi_a \leq \pi/2$ are satisfied. In this case, each impulse will affect the perigee height only, which decreases the fuel consumption but increases the de-orbit time. Figure 6 shows the active arc of the orbit near the apogee point.

If the debris removal mission assumes transfer of the captured debris object to a higher graveyard orbit, the tug's thrust should be turned on near the apogee and near the perigee of the current orbit to increase both the apogee and perigee. In this case, the "active arcs" of the orbit are

$$R \geq R_a - \Delta R_a \quad \text{or} \quad R \geq R_p - \Delta R_p, \qquad \Delta R_a > 0, \qquad \Delta R_p > 0 \tag{3}$$

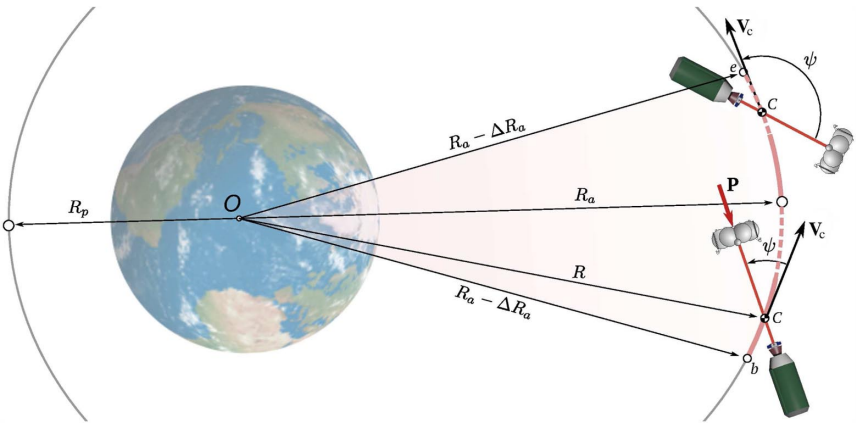

Fig. 6 Active phase of the de-orbit process.

Downloaded by MCMASTER UNIVERSITY on September 28, 2019 | http://arc.aiaa.org | DOI: 10.2514/1.G004615

where ΔR_p is the maximum difference between the perigee radius of the osculating orbit and radius of the current position of the system that denotes boundaries of the "active arc" near the perigee.

III. Model

A. Kinematics

The considered tug–debris system is presented in Fig. 7. The system consists of the space tug, tether, ADM, and space debris object. It is supposed that ADM is docked with the debris object, and so these bodies can be considered as a single object that we named as "debris."

The following assumptions are made:

1) Only the in-plane motion of the system is considered.

2) The system is orbiting around the Earth under the action of the central gravitational force of the Earth and tug's thrust only.

3) The tether A_1A_2 is a massless spring with the stiffness c_t and damping coefficient d_t.

4) The debris and space tug are considered to be rigid bodies.

The C_1 point in Fig. 7 is the center of mass of the space tug, and C_2 is the center of mass of the debris object (debris + ADM). Point C denotes the center of mass of the whole system. The motion of the system is considered relative to the Earth-centered inertial frame OX_0Y_0. The orientation of the tether is defined in the local-vertical-local, horizontal frame of the center of mass of the system Cx_oy_o. The position of the local-vertical, local-horizontal frame relative to the Earth-centered inertial frame OX_0Y_0 is defined by the distance R from the Earth center to the center of mass of the system C and the angle ϑ. The configuration of the system is described by six variables, $\boldsymbol{q} = [R, \vartheta, \psi, \varphi_1, \varphi_2, l]$, where ψ is the orientation of the tether relative to the local vertical axis, φ_1 is the orientation of the space tug axis C_1x_1 relative to the tether, and φ_2 is the orientation of the debris axis C_2x_1 relative to the tether. It is supposed that the attachment points of the tether are lying on the longitudinal axis of the debris and tug, respectively.

The column vectors of the space tug ($\boldsymbol{R}_1$) and space debris ($\boldsymbol{R}_2$) positions relative to the center of the Earth are

$$\boldsymbol{R}_1 = \boldsymbol{R} - \frac{m_2}{m}\boldsymbol{\rho}_{12}, \qquad \boldsymbol{R}_2 = \boldsymbol{R} + \frac{m_1}{m}\boldsymbol{\rho}_{12} \tag{4}$$

where $\boldsymbol{R}$ is the column vector of the center mass of the system in the OX_0Y_0 frame

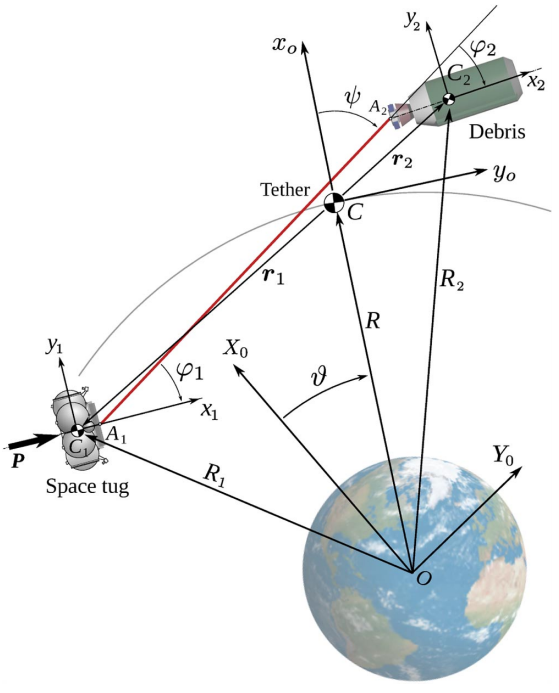

Fig. 7 Tethered tug–debris system.

$$\boldsymbol{R} = R\begin{bmatrix}\cos\vartheta\\ \sin\vartheta\end{bmatrix} \tag{5}$$

and $\boldsymbol{\rho}_{12} = \rightarrow C_1C_2$ is the column vector that connects the center of mass of the space tug with the center of mass of the debris. In the OX_0Y_0 frame, $\boldsymbol{\rho}_{12}$ is

$$\boldsymbol{\rho}_{12} = \begin{bmatrix} x_{c1}\cos\alpha_1 + x_{c2}\cos\alpha_2 + l\cos(\psi+\vartheta)\\ x_{c1}\sin\alpha_1 + x_{c2}\sin\alpha_2 + l\sin(\psi+\vartheta)\end{bmatrix} \tag{6}$$

where $x_{c1} = A_1C_1$ and $x_{c2} = A_2C_2$, $\alpha_1 = \varphi_1 + \psi + \vartheta$, $\alpha_2 = \varphi_2 + \psi + \vartheta$.

To build the motion equations of the system the tether attachment points vectors should be expressed as functions of $\boldsymbol{q}$. In the OX_0Y_0 frame the column vectors of the tether attachment points relative to the center of mass of the system are

$$\boldsymbol{r}_{A1} = \frac{1}{m}\begin{bmatrix} m_1x_{c1}\cos\alpha_1 - m_2(x_{c2}\cos\alpha_2 + l\cos(\psi+\vartheta))\\ m_1x_{c1}\sin\alpha_1 - m_2(x_{c2}\sin\alpha_2 + l\sin(\psi+\vartheta))\end{bmatrix} \tag{7}$$

$$\boldsymbol{r}_{A2} = \frac{1}{m}\begin{bmatrix} m_1(x_{c1}\cos\alpha_1 + l\cos(\psi+\vartheta)) - m_2x_{c2}\cos\alpha_2\\ m_1(x_{c1}\sin\alpha_1 + l\sin(\psi+\vartheta)) - m_2x_{c2}\sin\alpha_2\end{bmatrix} \tag{8}$$

The velocities of the space tug and debris object relative to the inertial frame OX_0Y_0 are

$$\boldsymbol{V}_1 = \frac{d\boldsymbol{R}}{dt} - \frac{m_2}{m}\frac{d\boldsymbol{\rho}_{12}}{dt}, \qquad \boldsymbol{V}_2 = \frac{d\boldsymbol{R}}{dt} + \frac{m_1}{m}\frac{d\boldsymbol{\rho}_{12}}{dt} \tag{9}$$

where

$$\frac{d\boldsymbol{R}}{dt} = \frac{dR}{dt}\begin{bmatrix}\cos\vartheta\\ \sin\vartheta\end{bmatrix} + R\frac{d\vartheta}{dt}\begin{bmatrix}-\sin\vartheta\\ \cos\vartheta\end{bmatrix} \tag{10}$$

and

$$\frac{d\boldsymbol{\rho}_{12}}{dt} = \begin{bmatrix} x_{c1}\omega_1\sin\alpha_1 - x_{c2}\omega_2\sin\alpha_2 + \dot{l}\cos(\psi+\vartheta) - l(\dot{\psi}+\dot{\vartheta})\sin(\psi+\vartheta)\\ x_{c1}\omega_1\cos\alpha_1 + x_{c2}\omega_2\cos\alpha_2 + \dot{l}\sin(\psi+\vartheta) + l(\dot{\psi}+\dot{\vartheta})\cos(\psi+\vartheta)\end{bmatrix} \tag{11}$$

where $\omega_1 = \dot{\varphi}_1 + \dot{\psi} + \dot{\vartheta}$, $\omega_2 = \dot{\varphi}_2 + \dot{\psi} + \dot{\vartheta}$.

B. Kinetic Energy of the System

Lagrange formalism is used to build the motion equations of the system

$$\frac{d}{dt}\frac{\partial T}{\partial \dot{q}_i} - \frac{\partial T}{\partial q_i} = Q_i, \qquad i = 1, \ldots, 6 \tag{12}$$

where T is the kinetic energy of the system and Q_i is the generalized force for the generalized coordinate q_i. Using expressions (4) and (9), the kinetic energy of the system can be expressed as

$$2T = \sum_{i=1}^{2}[m_i|\boldsymbol{V}_i|^2 + J_i\omega_i^2] \tag{13}$$

or in explicit form

$$2T = \sum_{i=1}^{2} m_i\left[\left(\dot{R}\sin\vartheta + R\dot{\vartheta}\cos\vartheta + (-1)^i\frac{m_{12}}{m_i}s_1\right)^2 + \left(\dot{R}\cos\vartheta - R\dot{\vartheta}\sin\vartheta + (-1)^i\frac{m_{12}}{m_i}s_2\right)^2\right] + \sum_{i=1}^{2}J_i\omega_i^2 \tag{14}$$

where $m_{12} = m_1m_2/m$ is the reduced mass of the system and

Downloaded by MCMASTER UNIVERSITY on September 28, 2019 | http://arc.aiaa.org | DOI: 10.2514/1.G004615

$$s_1 = x_{c1}\omega_1 \cos\alpha_1 + x_{c2}\omega_2 \cos\alpha_2 + \dot{l}\sin(\psi+\vartheta) + l(\dot{\psi}+\dot{\vartheta})\cos(\psi+\vartheta) \tag{15}$$

$$s_2 = -x_{c1}\omega_1 \sin\alpha_1 - x_{c2}\omega_2 \sin\alpha_2 + \dot{l}\cos(\psi+\vartheta) - l(\dot{\psi}+\dot{\vartheta})\sin(\psi+\vartheta) \tag{16}$$

C. Forces

In this subsection, the expressions for the generalized forces are presented. The system is orbiting under the action of the gravity force $\boldsymbol{G}_i$ acting on each body and the tug's thruster force $\boldsymbol{P}$. The space tug and debris are connected by the elastic tether. The tension force $\boldsymbol{T}$ of the tether depends on the tether length l. The gravity forces are

$$\boldsymbol{G}_i = -\mu\frac{m_i\boldsymbol{R}_i}{R_i^3}, \qquad i = 1,2 \tag{17}$$

where μ is the gravitational parameter of the Earth. The generalized forces Q_{Gj} corresponding to the gravity forces are

$$Q_{Gj} = \sum_{i=1}^{2}\frac{\partial \boldsymbol{R}_i}{\partial q_j}\cdot\boldsymbol{G}_i, \qquad j = 1,\ldots,6 \tag{18}$$

The generalized forces for the tug's thrust are

$$Q_{Pj} = \frac{\partial \boldsymbol{R}_1}{\partial q_j}\cdot\boldsymbol{A}_1\boldsymbol{e}_{1x}P, \qquad j = 1,\ldots,6 \tag{19}$$

where $\boldsymbol{e}_{1x} = [1,0]^T$ is the unit vector of the direction of the tug's thrust force in the tug's frame $C_1x_1y_1$, and $\boldsymbol{A}_1$ is the matrix that transforms coordinates from the tug's frame to the inertial frame:

$$\boldsymbol{A}_1 = \begin{bmatrix}\cos\alpha_1 & -\sin\alpha_1\\ \sin\alpha_1 & \cos\alpha_1\end{bmatrix} \tag{20}$$

Tether tension force $\boldsymbol{T}$ depends on the tether length. The tension force acts on the debris and space tug. Generalized forces corresponding to the tether tension force are

$$Q_{Tj} = \sum_{i=1}^{2}(-1)^{i-1}\frac{\partial \boldsymbol{R}_{Ai}}{\partial q_j}\cdot\boldsymbol{e}_t\cdot T(l)\cdot H(l) \tag{21}$$

where $\boldsymbol{e}_t$ is the unit vector aligned with the tether and directed from A_1 to A_2:

$$\boldsymbol{e}_t = \frac{\boldsymbol{R}_{A2}-\boldsymbol{R}_{A1}}{l} \tag{22}$$

Tether length is

$$l = |\boldsymbol{R}_{A2}-\boldsymbol{R}_{A1}| \tag{23}$$

$T(l)$ is the tether tension force:

$$T(l) = c_t(l-l_0) + \dot{l}d_t \tag{24}$$

$H(l)$ is the step function:

$$H(l) = \begin{cases}0, & l \le l_0\\ 1, & l > l_0\end{cases} \tag{25}$$

l_0 is the free length of the tether. The right side of the equations gets the form

$$Q_j = Q_{Gj} + Q_{pj} + Q_{Tj}, \qquad j = 1,\ldots,6 \tag{26}$$

Substituting Eqs. (14) and (26) into Eq. (12) gives the motion equations for the considered system. These equations are cumbersome and not presented here, but present no obstacle for a software package such as Maple or Mathematica.

D. Simplified Model

In this section, the simplified model of the tethered tug–debris system is considered. The model can be used to estimate the required angular velocity of the system that keeps the tether taut for any masses of the space tug and debris and the tug's thrust.

To derive the simplified equations the following assumptions are adopted:

1) The debris and space tug do not oscillate relative to the tether.
2) The debris and space tug are considered as point masses attached to the tether ($x_{c1} = x_{c2} = 0$).
3) The tension force of the tether T depends only on the elongation of the tether.
4) The tether is always taut ($l > l_0$).

The motion of the system is considered relative to the noninertial frame Cx_cy_c. The origin of the frame is placed in the center of mass of the system C. The scheme of the system is presented in Fig. 8. The tethered tug–debris system rotates around the center of mass C with the angular rate of $\omega = \dot{p}si$. The orientation of the tether relative to the frame Cx_oy_o is defined by the angle ψ. The motion of the space tug along the Cx_c axis of the frame Cx_cy_c can be described by the equation

$$m_1\frac{d^2l_1}{dt^2} = -P - T + \Phi_P + \Phi_\omega \tag{27}$$

where $\Phi_P = m_1a_c$ is the inertial force caused by the acceleration of the center of mass of the system under the action of the tug's thrust

$$a_c = \frac{P}{m_1+m_2} \tag{28}$$

$\Phi_\omega = m_1\omega^2l_1$ is the centrifugal force caused by rotation of the tethered tug–debris system relative to the center of mass, and $T = c_t(l-l_0)$ is the tension of the tether. The distance from the center of mass of the system to the space tug can be expressed as

$$l_1 = l\frac{m_2}{m_1+m_2} \tag{29}$$

Equation (27) can be rewritten as

$$\frac{d^2l}{dt^2} = \omega^2l - \frac{P}{m_1} - k^2(l-l_0) \tag{30}$$

where $k^2 = c_t/m_{12}$.

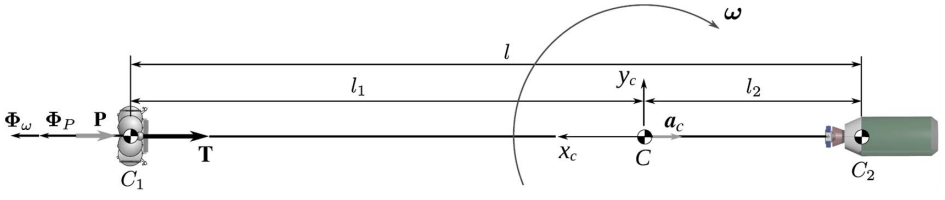

Fig. 8 Model of the tethered tug–debris system.

Downloaded by MCMASTER UNIVERSITY on September 28, 2019 | http://arc.aiaa.org | DOI: 10.2514/1.G004615

Leaving out of account the action of the gravitational torque acting on the tethered tug–debris system and supposing that the tug's thrust is applied along the tether, we can use the angular momentum equation

$$J\frac{d\omega}{dt} = 0 \tag{31}$$

where J is the moment of inertia of the system relative to the center of mass C:

$$J = l_1^2 m_1 + l_2^2 m_2 = m_{12} l^2 \tag{32}$$

Let us suppose that the tethered tug–debris system had the initial angular rate of ω_0 and the initial length of the tether is equal to its free length l_0. In this case, we can write

$$J_0\omega_0 = J\omega \Rightarrow \omega = \omega_0\frac{l_0^2}{l^2} \tag{33}$$

where $J_0 = m_{12}l_0^2$. Using Eq. (33), Eq. (30) gets the form

$$\frac{d^2l}{dt^2} = \omega_0^2\frac{l_0^4}{l^3} - \frac{P}{m_1} - k^2(l - l_0) \tag{34}$$

Introducing new variable $u = dl/dt$, we get

$$\int_{u_a}^{u_b} u\,du = \int_{l_a}^{l_b}\left(\omega_0^2\frac{l_0^4}{l^3} - \frac{P}{m_1} - k^2(l - l_0)\right)\mathrm{d}l \tag{35}$$

which allows us to obtain the first integral:

$$u_b^2 - u_a^2 = l_0^4\omega_0^2\frac{l_b^2 - l_a^2}{l_a^2 l_b^2} + k^2(l_a^2 - 2l_0l_a - l_b^2) + 2l_bk^2l_0 + 2\frac{P}{m_1}(l_a - l_b) \tag{36}$$

Equation (36) can be used to estimate the deformation of the tether during transient events when the tug's thrust P is turning "on" and "off." For example, for the tethered tug–debris system with the initial length $l_a = l_0$ that starts to rotate with the angular rate of ω_0, the maximum length of the tether l_b can be obtained from the equation

$$k^2l_b^4 - 2\,k^2l_0l_b^3 - (l_0^2\omega_0^2 - l_0^2k^2)l_b^2 + l_0^4\omega_0^2 = 0 \tag{37}$$

Equation (30) allows us to obtain the expression for the stationary length of the tether. For $d^2l/dt^2 = 0$ we get

$$l_s = \frac{k^2l_0 - P/m_1}{k^2 - \omega^2} \tag{38}$$

Taking into account Eq. (33), nonlinear Eq. (38) can be rewritten as

$$l_s^4 - \left(l_0 - \frac{P}{m_1k^2}\right)l_s^3 - \frac{\omega_0^2}{k^2}l_0^4 = 0 \tag{39}$$

Equation (39) allows us to get the stationary length of the tether $l_s = l_{sp}$ that starts to rotate with the angular rate of ω_0 with the initial length equal to the free length l_0 under the action of the tug's thrust P. For $P = 0$ one can get stationary tether length $l_s = l_{s0}$ for the same initial conditions when tug's propulsion system is in "off" state:

$$l_s^4 - l_0l_s^3 - \frac{\omega_0^2}{k^2}l_0^4 = 0 \tag{40}$$

The solutions of Eqs. (39) and (40) can be found for particular values of l_0, ω_0, and k. If the tether of length l_{s0} rotates with the angular rate $\omega_0^s = \omega_0 l_0^2/(l_{s0})^2$, then applying the tug's thrust force P will decrease the length of the tether to the value $l_{\min}$. $l_{\min}$ can be obtained from the fourth-order equation

$$-\frac{1}{2}k^2l_{\min}^4 + l_{\min}^3\left(k^2l_0 - \frac{P}{m_1}\right) + \frac{1}{2}l_{\min}^2\left(\frac{2Pl_{s0}}{m_1} + k^2l_{s0}(l_{s0} - 2l_0) + \frac{l_0^4\omega_0^2}{l_{s0}^2}\right) - \frac{1}{2}l_0^4\omega_0^2 = 0 \tag{41}$$

This length should be greater than the free length of the tether:

$$l_{\min} > l_0 \tag{42}$$

If the tether of length l_{sp} rotates with the angular rate $\omega_0^s = \omega_0 l_0^2/(l_{sp})^2$ and the tug's propulsion system is in "on" state, then turning "off" the thrust force will increase the length of the tether to the value $l_{\max}$, which can be obtained from the equation

$$k^2l_0l_{\max}^3 - \frac{1}{2}k^2l_{\max}^4 + \frac{1}{2}l_{\max}^2\left(k^2l_{sp}(l_{sp} - 2l_0) + \frac{l_0^4\omega_0^2}{l_{sp}^2}\right) - \frac{1}{2}l_0^4\omega_0^2 = 0 \tag{43}$$

This value can be used to estimate the tether strength:

$$(l_{\max} - l_0)k < \sigma^*A \tag{44}$$

where σ^* is the tensile strength of the tether and A is the cross-sectional area of the tether.

E. Tug's Thrust Control

Applying tug's thrust along the tether can increase the oscillation amplitude of the tether that affects the oscillations of the debris and space tug relative to the tether.

To decrease the oscillation amplitude of the tether the control system of the space tug should damp the tether oscillation. We propose to use a simple, well-known control algorithm to do this. It is supposed that the tug's thrust is a discrete quantity. The tug's thrust can be in "on" or "off" state. In the previous subsection we obtained two stable solutions for the tether length, Eqs. (39) and (40). We propose to use the following control law when the tug's thrust is on the "active arc" of the orbit and when $\cos\psi \geq \cos\psi_a$ (Fig. 9):

$$u_p^{\text{on}} = \begin{cases} 0 & l < l_{sp} + \delta l \text{ and } \dot{l} < -\delta v \\ 1 & \text{othercases} \end{cases} \tag{45}$$

where δl and δv are threshold values for the tether length and elongation velocity. The generalized forces for the tug's thrust are (Fig. 10)

$$Q_{Pj} = \frac{\partial \boldsymbol{R}_1}{\partial q_j}\cdot \boldsymbol{A}_1\boldsymbol{e}_{1x}Pu_p^{\text{on}}, \qquad j = 1, \ldots, 6 \tag{46}$$

When the tug's thrust should be turned off (on the "passive arc" of the orbit) the generalized forces for the tug's thrust are

$$Q_{Pj} = \frac{\partial \boldsymbol{R}_1}{\partial q_j}\cdot \boldsymbol{A}_1\boldsymbol{e}_{1x}Pu_p^{\text{off}}, \qquad j = 1, \ldots, 6 \tag{47}$$

where

$$u_p^{\text{off}} = \begin{cases} 1 & l > l_{s0} + \delta l \text{ and } \dot{l} > \delta v \\ 0 & \text{othercases} \end{cases} \tag{48}$$

Now we can write the control algorithm for the tug's thrust for de-orbit mission in the following form:

$$Q_{Pj} = \frac{\partial \boldsymbol{R}_1}{\partial q_j}\cdot \boldsymbol{A}_1\boldsymbol{e}_{1x}Pu_p, \qquad j = 1, \ldots, 6 \tag{49}$$

where

$$u_p = \begin{cases} u_p^{\text{on}} & R > R_a - \Delta R_a \wedge \cos\psi > \cos\psi_a \wedge 0 < \psi < \pi/2 \\ u_p^{\text{off}} & \text{othercases} \end{cases} \tag{50}$$

F. Initial Rotation of the Tether

The required rotation of the tethered tug–debris system can be achieved through the initial relative motion of the space tug relative to the debris object. The space tug should be injected into the interception orbit with the desired difference between the orbital velocity of the debris and space tug in the final approach point. In that point, the space tug and space debris have to be connected by the tether (Fig. 11).

To form the tethered connection the space tug can deploy the net on the trajectory of the space debris. Here we consider using ADM for delivering the tether from the space tug to the debris.

It is supposed that the space tug and debris are orbiting in the same plane. The space debris is orbiting in a circular orbit with the radius R_{deb}. The space tug with ADM is orbiting in an elliptical orbit $R_{\text{tug}} \times R_{\text{deb}} - l_0$. The elliptical orbit of the space tug can be formed by single impulse maneuver from the base circular orbit of the space tug with the height R_{tug}. In the approach point, the space tug has the velocity V_1, which is less than the velocity of the debris object, V_2. So if in the final point the tug and debris are connected by the tether, the angular velocity of the system can be calculated as

$$\omega_0 = \frac{V_2 - V_1}{l_0} = \frac{1}{l_0}\left[\sqrt{\frac{\mu}{R_{\text{deb}}}} - \sqrt{2\mu R_{\text{tug}}\left(\frac{R_{\text{tug}}}{R_{\text{deb}} - l_0} + 1\right)}\frac{1}{R_{\text{tug}} + R_{\text{deb}} - l_0}\right] \tag{51}$$

To establish the tethered connection between the debris and the space tug, the ADM with the tether should be separated from the space tug near the approach point. Figure 11 shows stages of the tethered tug–debris system formation. The ADM separates from the space tug at the point $\boldsymbol{R}_1(0)$. The position of the ADM relative to the Earth-centered OX_0Y_0 frame is described by the vector $\boldsymbol{R}_3$. At the approach point the position and velocity of the ADM $(\boldsymbol{R}_3, \boldsymbol{V}_3)$ should be equal to the position and velocity of the debris object $(\boldsymbol{R}_2, \boldsymbol{V}_2)$ and the distance between the tug and debris should be equal to l_0.

We use a simple terminal state vector control [31] to build program control for the ADM. The control acceleration of autonomous module can be written as

$$\boldsymbol{u}_3(t) = \frac{\mu}{R_3^3}\boldsymbol{R}_3 + \frac{6(\boldsymbol{R}_2(t_k) - (\boldsymbol{R}_3 + \boldsymbol{V}_2(t_k)(t_k - t)))}{(t_k - t)^2} + \frac{4(\boldsymbol{V}_2(t_k) - \boldsymbol{V}_3)}{t_k - t}, \qquad 0 \le t < t_k \tag{52}$$

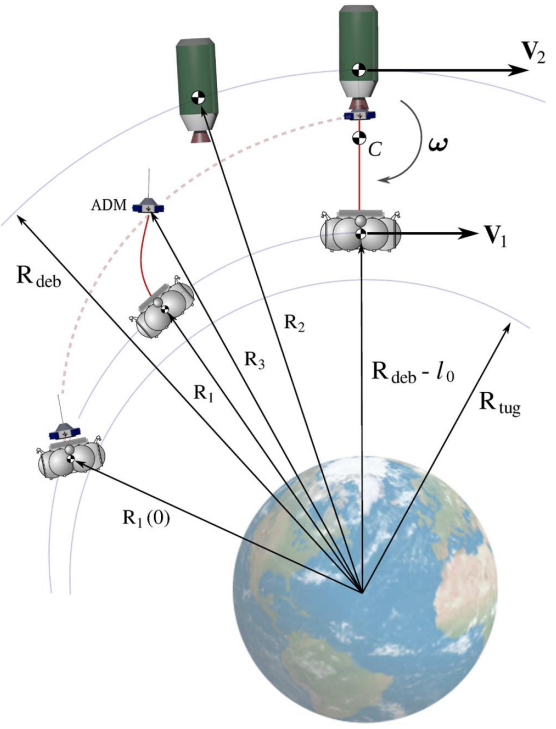

Fig. 11 Interception of the space debris object.

where $\boldsymbol{R}_3$ is the column vector of the ADM relative to the Earth-centered inertial frame OX_0Y_0, $\boldsymbol{V}_3$ is the velocity vector of the ADM relative to the OX_0Y_0 frame, and $\boldsymbol{R}_2(t_k)$ and $\boldsymbol{V}_2(t_k)$ are the final position vector and final velocity vector of the debris object. The initial conditions are $t = 0$, $\boldsymbol{R}_1(0) = \boldsymbol{R}_3(0)$, and $\boldsymbol{V}_1(0) = \boldsymbol{V}_3(0)$.

IV. Simulation

In this section we consider two simulation cases that illustrate the proposed method for de-orbiting the space debris and for transferring the debris to a graveyard orbit. In both cases the debris object is orbiting in a circular orbit with a height of 800 km. The space tug is orbiting in the same orbital plane with a perigee height of 700 km and an apogee height of 795 km. The simulation results are obtained using mathematical model that is presented in Secs. III.A–III.C. It is supposed that the space tug attitude control system maintains the alignment between the space tug body and tether $\varphi_1 = 0$. The oscillation amplitude of the debris relative to the tether depends on the initial relative velocity between the debris and space tug, initial length of the tether, and the initial angular velocity of the debris. The oscillation of the debris can be damped using different control techniques [32–36]. Here we do not consider this aspect of the active debris removal problem.

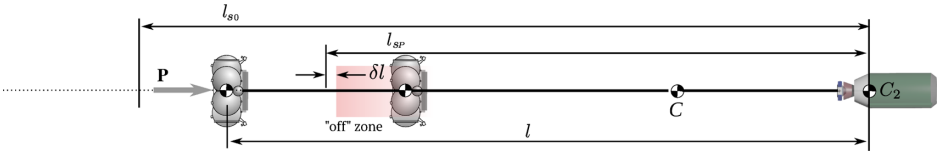

Fig. 9 "Off" zone of the tug's thrust during the active phase.

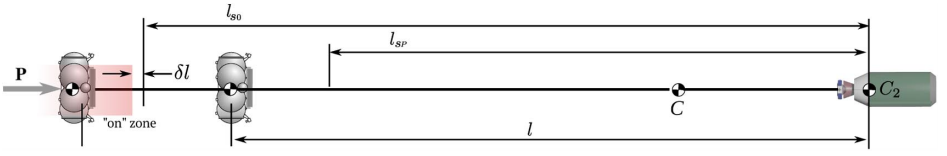

Fig. 10 "On" zone of the tug's thrust during the passive phase.

Downloaded by MCMASTER UNIVERSITY on September 28, 2019 | http://arc.aiaa.org | DOI: 10.2514/1.G004615

Table 1 Parameters of the system

Parameter	Value	Parameter	Value
Space tug mass, m_1	2,500 kg	Debris orbit	800×800 km
Space tug inertia, J_{1z}	5,000 kg $\cdot$ m^2	Tug's orbit	700×795 km
Space debris mass, m_2	1,500 kg	ADM mass, m_3	200 kg
Space debris inertia, J_2	10,000 kg $\cdot$ m^2	$x_{c1} = x_{c2}$	1 m
Tether stiffness, c_t	377 N/m	Tether damping, k_t	0
Tether free length, l_0	5,000 m	Tether density, ρ	1.44 g/cm^3
δl	0.1 m	δv	0.1 m/s
Space tug thrust, P	2,000 N	$\Delta R_a = \Delta R_p$	10 km

A. Parameters of the System and Initial Conditions

The space debris is a upper-stage-type debris with mass of 1500 kg. The space tug has a mass of 2500 kg. The tether length is 5000 m. The tether is made of 3-mm-diam Kevlar wire with the elastic modulus $E = 80$ GPa and tensile strength $\sigma^* = 3.6$ GPa [37]. This tether has a mass of 51 kg. Parameters of the considered system are presented in Table 1.

B. Simulation Results

1. Interception

At the first stage, ADM separates from the space tug for intercepting the space debris object. We suppose that the space tug has already synchronized its orbital motion with the motion of the debris object, and so the space tug passes the apogee of the orbit when the arguments of the latitude of the tug and debris are the same. ADM separates from the tug $t_f = 300$ s before the point of closest distance between the tug and debris. The ADM separates from the space tug when the distance to the debris object is of 6 km along track and 10 km in the radial direction. Figure 12 shows the trajectory of the tug (solid line) and ADM (dashed line) relative to the debris object in the local-vertical, local-horizontal frame of the debris. The arrows in Fig. 12 denote the control acceleration of the autonomous docking module in the OX_0Y_0 frame. The projections of the control acceleration in the local-vertical, local-horizontal frame of the debris object are presented in Fig. 13. Figure 14 shows the distance between the autonomous docking module and space debris object.

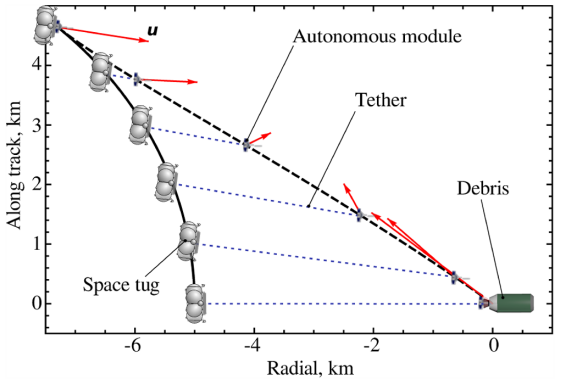

Fig. 12 Trajectories of the tug and ADM relative to the debris object.

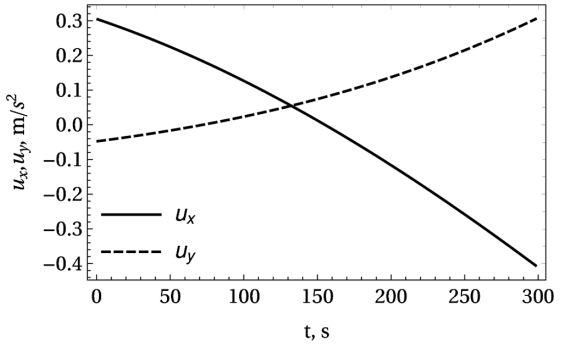

Fig. 13 Control acceleration of the ADM.

Using the control acceleration of the ADM (Fig. 13), one can estimate the propellant consumption for the interception phase:

$$m_{f3} = \int_0^{t_f} \frac{|\boldsymbol{u}_3| m_3}{I_{3\,s}}\,\mathrm{d}t \tag{53}$$

where I_{3s} is the specific impulse of the ADM propulsion system. For $I_{3\,s} = 3000$ m/s we get $m_{f3} < 4.5$ kg.

The initial angular rate of the tethered tug–debris is $\omega_0 = 0.256$ deg/s. The tension of the tether for this angular rate is less than tug's thrust force $T = 100$ N $< P = 2000$ N. To increase the tension force the tether length should be decreased by the tether control system. Here we consider decreasing the tether length from 5000 m to 1500 m. In this case the angular rate increases up to $\omega_0 = 2.84$ deg/s and the tension of the tether increases up to $T = 3668$ N, which is greater than the tug's thrust. The stationary length of the tether for $P = 0$ is $l_{s0} = 1509.7$ m and $l_{sp} = 1507.6$ m for $P = 2000$ N.

2. Transfer to the Graveyard Orbit

The first simulation case illustrates the transfer of the debris object from the LEO orbit to the graveyard orbit above 2000 km. This scenario can be used to transfer dangerous debris objects that cannot be de-orbited to the Earth's atmosphere.

Figure 15 shows the time history of the apogee and perigee height of the tug–debris system orbit. The apogee and perigee of the orbit

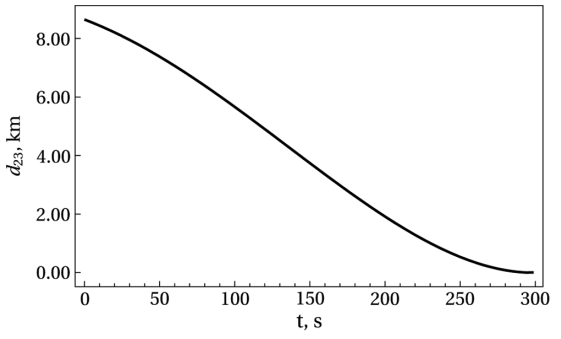

Fig. 14 Distance between the ADM and debris.

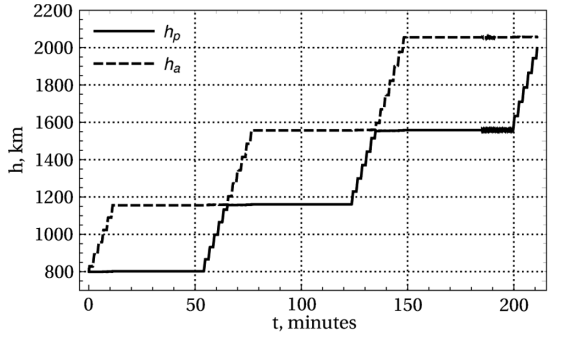

Fig. 15 Apogee and perigee of the orbit during the transfer to the graveyard orbit.

Downloaded by MCMASTER UNIVERSITY on September 28, 2019 | http://arc.aiaa.org | DOI: 10.2514/1.G004615

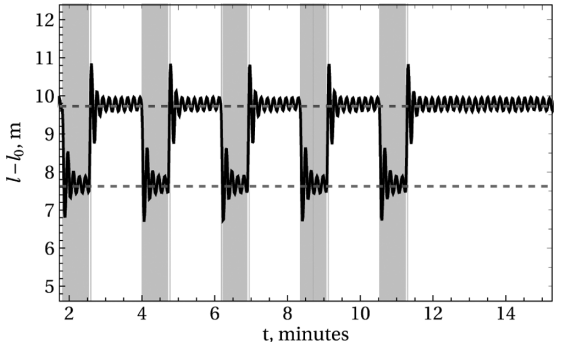

Fig. 16 Time history of the tether elongation.

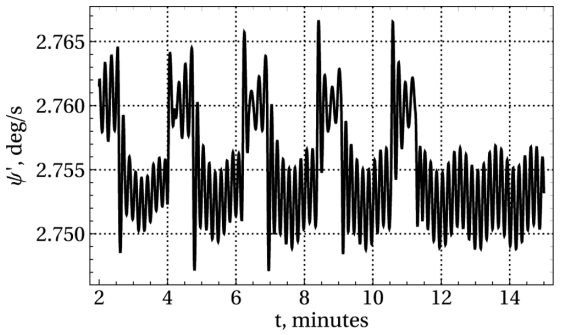

Fig. 17 Angular velocity of the tether.

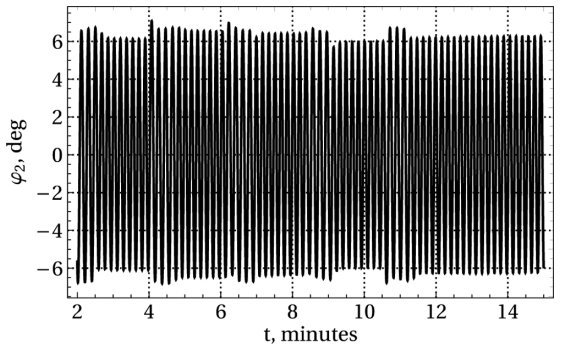

Fig. 18 Time history of the angle φ_2.

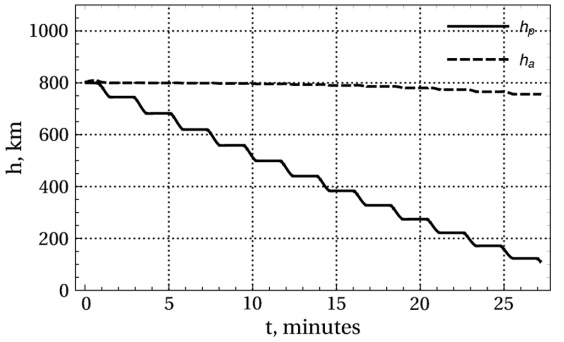

Fig. 19 Apogee and perigee of the orbit.

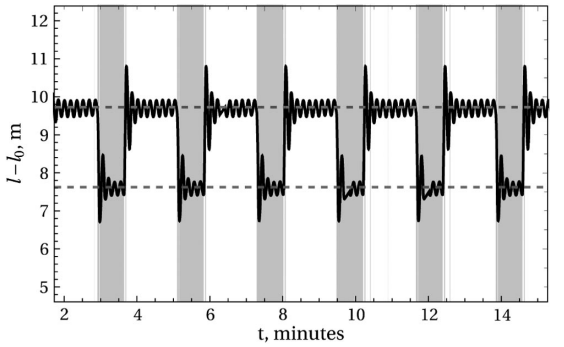

Fig. 20 Elongation of the tether.

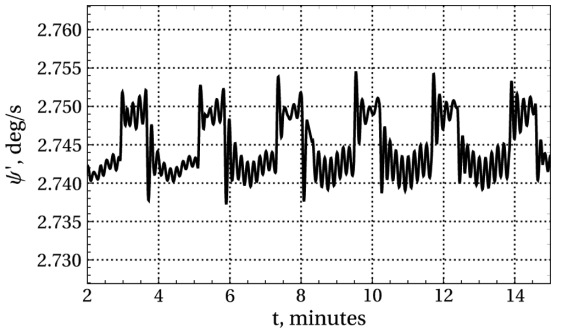

Fig. 21 Angular rate of the tethered tug–debris system.

are changing stepwise because the tug's thrust is "on" near the perigee and near the apogee only ($R > R_a - \Delta R_a \vee R < R_p + \Delta R_p$). Figure 16 shows the time history of the tether elongation $(l - l_0)$ in the time interval from 0 to 20 min when the thrust P is applied periodically to the space tug near the perigee of the orbit. Figure 16 illustrates that the tether remains taut during the de-orbit process ($l > l_0$) and the tensile strength does not exceed $\sigma^* = 3.6$ GPa:

$$\frac{4(l_{\max} - l_0)k}{\pi d^2} \approx \frac{4 \cdot 11 \text{ m} \cdot 377 \text{ N/m}}{\pi(0.003 \text{ m})^2} \approx 0.6 \text{ GPa} < 3.6 \text{ GPa} \quad (54)$$

Gray vertical bars on the graph indicate the intervals when the tug's thrust is turned "on."

Figure 16 also illustrates that the proposed control for the space tug's thrust damps oscillations of the tether. Figure 17 shows the angular velocity of the tug–debris system $\dot{\psi}$. The angular velocity is changing periodically due to the change in the tether length under the action of the tug's thrust.

Figure 18 shows the time history of the angle φ_2, which indicates the oscillations of the debris body relative to the tether. The figure shows the change of the angle in the interval $t < 20$ min. The maximum value of the angle φ_2 during the de-orbit process does not exceed 4 deg.

C. De-Orbit

Figures 19–21 show the simulations results for the case when the space tug de-orbits the debris object. The space tug applies the de-orbit impulses when the angle between the orbital velocity vector of the system and the tug's thrust vector is greater than $3\pi/2$ and when the tug's height is $R(t) \geq R_a - \Delta R_a$.

Figure 19 shows the time history of the apogee and perigee of the system's orbit. The apogee changes slightly but the perigee of the orbit changes stepwise. The space tug decreases the perigee height as low as 100 km.

Figure 20 shows the elongation of the tether during the first 20 min of the de-orbit process. Tether's elongation behavior during the de-orbit process does not differ from the tether elongation behavior during the transfer to the graveyard orbit. Elongation of the tether is greater than zero.

Figure 21 shows the time history of the angular rate of the system. As in the previous case we see the intervals where the angular rate is increased due to the action of the tug's thrust that decreases tether's length and increases the angular rate.

V. Conclusions

The obtained results show that centrifugal inertia forces in the rotating tethered tug–debris system allow applying tug's thrust along the tether in the direction to compress it. The angular rate of the

Downloaded by MCMASTER UNIVERSITY on September 28, 2019 | http://arc.aiaa.org | DOI: 10.2514/1.G004615

tethered tug–debris system has to ensure that the tension of the tether does not fall below zero during the transient events associated with the turning "on" and "off" the tug's thrust. Required rotation of the tethered tug–debris system can be achieved by the relative orbital motion of the debris object and the space tug by using the ADM to deliver the tether from the space tug to space debris. Using the ADM reduces the requirements on the space tug control system. To de-orbit the tethered debris object the tug's thrust should be turned "on" when the projection of the tug's thrust on the orbital velocity vector of the system is negative. The simulation results show that an orbital-stage-type debris object with a mass about 1500 kg can be de-orbited by the space tug with a mass of 2500 kg and thrust level of 2000 N in 30 min. The proposed technique can be used with various stiff and nonstiff capture devices like nets or harpoons, robotic arms, and probe-cone docking devices. The proposed technique can be used during the design of the first orbital experiment for active debris removal as a piggyback mission using the existing upper stages (Fregat, Briz, etc.) as the space tug and using the ADM as the piggyback small spacecraft for capturing a selected space debris object.

Downloaded by MCMASTER UNIVERSITY on September 28, 2019 | http://arc.aiaa.org | DOI: 10.2514/1.G004615

Acknowledgments

This research was supported by a grant (No. 9.1023.2017 PCH) from the Ministry of Education and Science of the Russian Federation, "Improvement of Environmental Safety and Economic Efficiency of Launch Vehicles with Main Liquid Rocket Engines."

References

[1] Anselmo, L., and Pardini, C., "Ranking Upper Stages in Low Earth Orbit for Active Removal," *Acta Astronautica*, Vol. 122, May–June 2016, pp. 19–27. doi:10.1016/j.actaastro.2016.01.019

[2] Pardini, C., and Anselmo, L., "Evaluating the Environmental Criticality of Massive Objects in LEO for Debris Mitigation and Remediation," *Acta Astronautica*, Vol. 145, April 2018, pp. 51–75. doi:10.1016/j.actaastro.2018.01.028

[3] Iess, L., Bruno, C., Ulivieri, C., Ponzi, U., Parisse, M., Laneve, G., Vannaroni, G., Dobrowolny, M., De Venuto, F., and Bertotti, B., et al., "Satellite De-Orbiting by Means of Electrodynamic Tethers Part I: General Concepts and Requirements," *Acta Astronautica*, Vol. 50, No. 7, 2002, pp. 399–406. doi:10.1016/S0094-5765(01)00180-1

[4] Castronuovo, M. M., "Active Space Debris Removal—A Preliminary Mission Analysis and Design," *Acta Astronautica*, Vol. 69, Nos. 9–10, 2011, pp. 848–859. doi:10.1016/j.actaastro.2011.04.017

[5] Schaub, H., and Moorer, D. F., "Geosynchronous Large Debris Reorbiter: Challenges and Prospects," *Advances in the Astronautical Sciences*, Vol. 139, AIAA, Reston, VA, 2011, pp. 163–179. doi:10.1007/s40295-013-0011-8

[6] Kitamura, S., Hayakawa, Y., and Kawamoto, S., "A Reorbiter for Large GEO Debris Objects Using Ion Beam Irradiation," *Acta Astronautica*, Vol. 94, No. 2, 2014, pp. 725–735. doi:10.1016/j.actaastro.2013.07.037

[7] Botta, E. M., Sharf, I., and Misra, A. K., "Contact Dynamics Modeling and Simulation of Tether Nets for Space-Debris Capture," *Journal of Guidance, Control, and Dynamics*, Vol. 40, No. 1, 2017, pp. 110–123. doi:10.2514/1.G000677

[8] Felicetti, L., Gasbarri, P., Pisculli, A., Sabatini, M., and Palmerini, G. B., "Design of Robotic Manipulators for Orbit Removal of Spent Launchers' Stages," *Acta Astronautica*, Vol. 119, Feb.–March 2016, pp. 118–130. doi:10.1016/j.actaastro.2015.11.012

[9] Van der Heide, E. J., and Kruijff, M., "Tethers and Debris Mitigation," *Acta Astronautica*, Vol. 48, Nos. 5–12, 2001, pp. 503–516. doi:10.1016/S0094-5765(01)00074-1

[10] Jasper, L. E. Z., Seubert, C. R., Schaub, H., Trushlyakov, V., and Yutkin, E., "Tethered Tug for Large Low Earth Orbit Debris Removal," *Advances in the Astronautical Sciences*, Vol. 143, Univelt Inc., San Diego, CA, 2012, pp. 2223–2242.

[11] Qi, R., Misra, A. K., and Zuo, Z., "Active Debris Removal Using Double-Tethered Space-Tug System," *Journal of Guidance, Control, and Dynamics*, Vol. 40, No. 3, 2016, pp. 1–9. doi:10.2514/1.G000699

[12] Aslanov, V. S., and Yudintsev, V. V., "The Motion of Tethered Tug-Debris System with Fuel Residuals," *Advances in Space Research*, Vol. 56, No. 7, 2015, pp. 1493–1501. doi:10.1016/j.asr.2015.06.032

[13] Cresto Aleina, S., Viola, N., Stesina, F., Viscio, M. A., and Ferraris, S., "Reusable Space Tug Concept and Mission," *Acta Astronautica*, Vol. 128, Aug. 2016, pp. 21–32. doi:10.1016/j.actaastro.2016.07.003

[14] Aslanov, V. S., and Ledkov, A. S., "Attitude Motion of Cylindrical Space Debris During Its Removal by Ion Beam," *Mathematical Problems in Engineering*, Vol. 2017, Nov. 2017, pp. 1–7. doi:10.1155/2017/1986374

[15] Merino, M., Ahedo, E., Bombardelli, C., Urrutxua, H., and Peláez, J., "Ion Beam Shepherd Satellite for Space Debris Removal," *4th European Conference for Aerospace Sciences*, Vol. 1, No. 3, 2011, pp. 1–8. doi:10.2514/1.51832

[16] Schaub, H., and Sternovsky, Z., "Active Space Debris Charging for Contactless Electrostatic Disposal Maneuvers," *Advances in Space Research*, Vol. 53, No. 1, 2014, pp. 110–118. doi:10.1016/j.asr.2013.10.003

[17] Aslanov, V. S., "Gravitational Trap for Space Debris in Geosynchronous Orbit," *Journal of Spacecraft and Rockets*, Vol. 56, No. 4, 2019, pp. 1277–1281. doi:10.2514/1.a34384

[18] Shan, M., Guo, J., and Gill, E., "Review and Comparison of Active Space Debris Capturing and Removal Methods," *Progress in Aerospace Sciences*, Vol. 80, Jan. 2016, pp. 18–32. doi:10.1016/j.paerosci.2015.11.001

[19] Aslanov, V. S., and Yudintsev, V. V., "Dynamics of Large Space Debris Removal Using Tethered Space Tug," *Acta Astronautica*, Vol. 91, Oct.–Nov. 2013, pp. 149–156. doi:10.1016/j.actaastro.2013.05.020

[20] Lavagna, M., Armellin, R., Bombelli, A., Benvenuto, R., and Carta, R., "Debris Removal Mechanism Based on Tethered Nets," *Proceedings of i-SAIRAS 2012*, 2012, pp. 1–6.

[21] Cercos, L., Stefanescu, R., Medina, A., Benvenuto, R., Lavagna, M., Gonzalez, I., Rodriguez, N., and Wormnes, K., "Validation of a Net Active Debris Removal Simulator Within Parabolic Flight Experiment," *12th International Symposium on Artificial Intelligence, Robotics and Automation in Space*, 2014, p. 8.

[22] Zhai, G., Zhang, J.-R., and Yao, Z., "Circular Orbit Target Capture Using Space Tether-Net System," *Mathematical Problems in Engineering*, Vol. 2013, 2013, Paper 601482. doi:10.1155/2013/936375

[23] Dudziak, R., Tuttle, S., and Barraclough, S., "Harpoon Technology Development for the Active Removal of Space Debris," *Advances in Space Research*, Vol. 56, No. 3, 2015, pp. 509–527. doi:10.1016/j.asr.2015.04.012

[24] Jasper, L., and Schaub, H., "Input Shaped Large Thrust Maneuver with a Tethered Debris Object," *Acta Astronautica*, Vol. 96, No. 1, 2014, pp. 128–137. doi:10.1016/j.actaastro.2013.11.005

[25] Decou, A. B., "Tether Static Shape for Rotating Multimass, Multitether, Spacecraft for "Triangle" Michelson Interferometer," *Journal of Guidance, Control, and Dynamics*, Vol. 12, No. 2, 1989, pp. 273–275. doi:10.2514/3.20401

[26] Palmerini, G. B., Sgubini, S., and Sabatini, M., "Space Webs Based on Rotating Tethered Formations," *Acta Astronautica*, Vol. 65, Nos. 1–2, 2009, pp. 131–145. doi:10.1016/j.actaastro.2009.01.056

[27] Trushlyakov, V. I., Shatrov, Y. T., Oleynikov, I. I., Makarov, Y. N., and Yutkin, E. A., "The Method of Docking Spacecraft and Device for Its Implementation," Patent RU 2521082, 2010.

[28] Trushlyakov, V. I., and Yudintsev, V. V., "Systems Engineering Design and Optimization of an Active Debris Removal Mission of a Spent Rocket Body Using Piggyback Autonomous Module," *3rd IAA Conference on Dynamics and Control of Space Systems (DYCOSS 2017)*, Univelt Inc., San Diego, CA, 2017, pp. 667–681.

[29] Lagno, O. G., Lipatnikova, T. I., Makarov, Y. N., Mironova, T. V., Trushlyakov, V. I., Shatrov, Y. T., and Yudintsev, V. V., "Parameters Design of Autonomous Docking Module and the Choice of Suitable Target and Primary Payload for ADR," *Proceedings of the 7th European Conference on Space Debris ESOC*, Vol. 7, European Space Operations Centre, Paris, France, 2017.

[30] Jones, H. M., Malaviarachchi, P., MacKenzie, A. C., Ficocelli, M., and Sprawson, G. W. F., "Spacecraft Docking Mechanism," U.S. Patent 6,969,030 B1, 2005.

[31] Battin, R. H., *An Introduction to the Mathematics and Methods of Astrodynamics*, rev. ed., AIAA, Reston, VA, 1999, pp. 559–566. doi:10.2514/4.861543

[32] Huang, P., Wang, D., Meng, Z., Zhang, F., and Guo, J., "Adaptive Postcapture Backstepping Control for Tumbling Tethered Space Robot-Target Combination," *Journal of Guidance, Control, and Dynamics*, Vol. 39, No. 1, 2016, pp. 150–156. doi:10.2514/1.G001309

[33] Hovell, K., and Ulrich, S., "Attitude Stabilization of an Uncooperative Spacecraft in an Orbital Environment Using Visco-Elastic Tethers," *2016 AIAA Guidance, Navigation, and Control Conference*, AIAA Paper 2016-0641, 2016.

[34] Peters, T. V., Briz Valero, J. F., Escorial Olmos, D., Lappas, V., Jakowski, P., Gray, I., Tsourdos, A., Schaub, H., and Biesbroek, R., "Attitude Control Analysis of Tethered De-Orbiting," *Acta Astronautica*, Vol. 146, May 2018, pp. 316–331. doi:10.1016/j.actaastro.2018.03.016

[35] Chu, Z., Di, J., and Cui, J., "Hybrid Tension Control Method for Tethered Satellite Systems During Large Tumbling Space Debris Removal," *Acta Astronautica*, Vol. 152, Nov. 2018, pp. 611–623. doi:10.1016/j.actaastro.2018.09.016

[36] Wang, B., Meng, Z., Jia, C., and Huang, P., "Anti-Tangle Control of Tethered Space Robots Using Linear Motion of Tether Offset," *Aerospace Science and Technology*, Vol. 89, June 2019, pp. 163–174. doi:10.1016/j.ast.2019.03.060

[37] Aslanov, V. S., and Ledkov, A. S., *Dynamics of Tethered Satellite Systems*, Woodhead Publ., Sawston, Cambridge, U.K., 2013, p. 64. doi:10.1017/CBO9781107415324.004

Downloaded by MCMASTER UNIVERSITY on September 28, 2019 | http://arc.aiaa.org | DOI: 10.2514/1.G004615